

NPS ARCHIVE  
1965  
JENKINS, G.

AN INVESTIGATION OF THE FEASIBILITY OF A  
METHOD FOR MEASURING THERMAL NEUTRON  
ABSORPTION CROSS SECTIONS USING  
THE AGN-201 REACTOR

GEORGE J. JENKINS  
HERBERT B. RICHTER











AN INVESTIGATION OF THE FEASIBILITY OF A METHOD  
FOR MEASURING THERMAL NEUTRON ABSORPTION CROSS SECTIONS  
USING THE AGN-201 REACTOR

by

George J. Jenkins, Jr.  
Lieutenant, United States Navy

and

Herbert B. Richter  
Lieutenant, United States Navy

Submitted in partial fulfillment of  
the requirements for the degree of

MASTER OF SCIENCE  
IN  
PHYSICS

United States Naval Postgraduate School  
Monterey, California

1 9 6 5

NPS ARCHIVE

~~JASS~~

1965

JENKINS, G.

AN INVESTIGATION OF THE FEASIBILITY OF A METHOD  
FOR MEASURING THERMAL NEUTRON ABSORPTION CROSS SECTIONS  
USING THE AGN-201 REACTOR

by

George J. Jenkins, Jr.

and

Herbert B. Richter

This work is accepted as fulfilling  
the thesis requirements for the degree of

MASTER OF SCIENCE  
IN  
PHYSICS

from the

United States Naval Postgraduate School



## ABSTRACT

The feasibility of measuring thermal neutron absorption cross section from the results of first-order reactor perturbation theory was investigated. Techniques were developed for this measurement utilizing the AGN-201 reactor of the U. S. Naval Postgraduate School.

These techniques were evaluated by measurement of the thermal absorption cross section of indium using gold-197 as a standard. The result obtained was

$$194.4 \pm 2.3 \text{ barns.}$$

A comparison with the most recently published value of this cross section,  $196 \pm 5$  barns, demonstrates the feasibility of the method for obtaining improved precision for the measurement of the cross sections of selected materials.



## TABLE OF CONTENTS

Section	Title	Page
1.	INTRODUCTION	1
2.	THEORY	2
3.	DESCRIPTION OF EXPERIMENTAL TECHNIQUES	6
	a) Reactivity Differences	6
	b) Ratio of Volume-averaged Thermal Fluxes	13
4.	RESULTS AND ERROR ANALYSIS	21
	a) Reactivity Measurements	21
	b) Ratio of the Volume-averaged Thermal Fluxes	23
	c) The 2,200 m/sec Microscopic Cross Section of Indium	23
5.	DISCUSSION AND CONCLUSIONS	26
6.	ACKNOWLEDGEMENTS	31
7.	BIBLIOGRAPHY	32

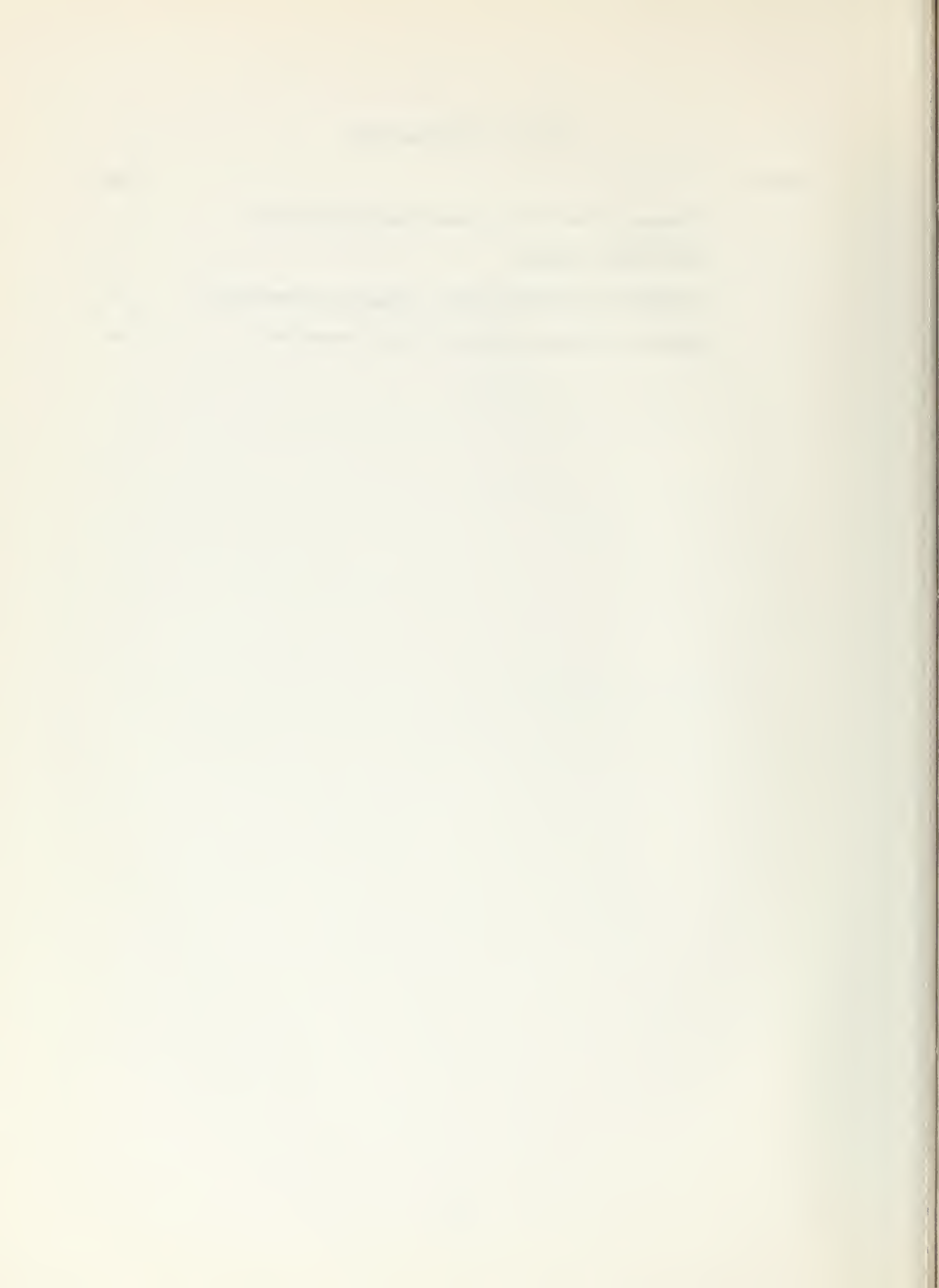
## Appendix

I.	Expression of Equation (6) in Terms of Experimentally Observable Parameters	33
II.	Computer Program for Reduction of Gold Activated Data	37



## LIST OF ILLUSTRATIONS

Figure		Page
1.	Diagram of the Circuit Measuring Decade Time	7
2.	The Holder Assembly	9
3.	Circuit for Measuring Small Changes in Temperature	12
4.	Specific Thermal Activity within Indium Foil	24



## 1. INTRODUCTION.

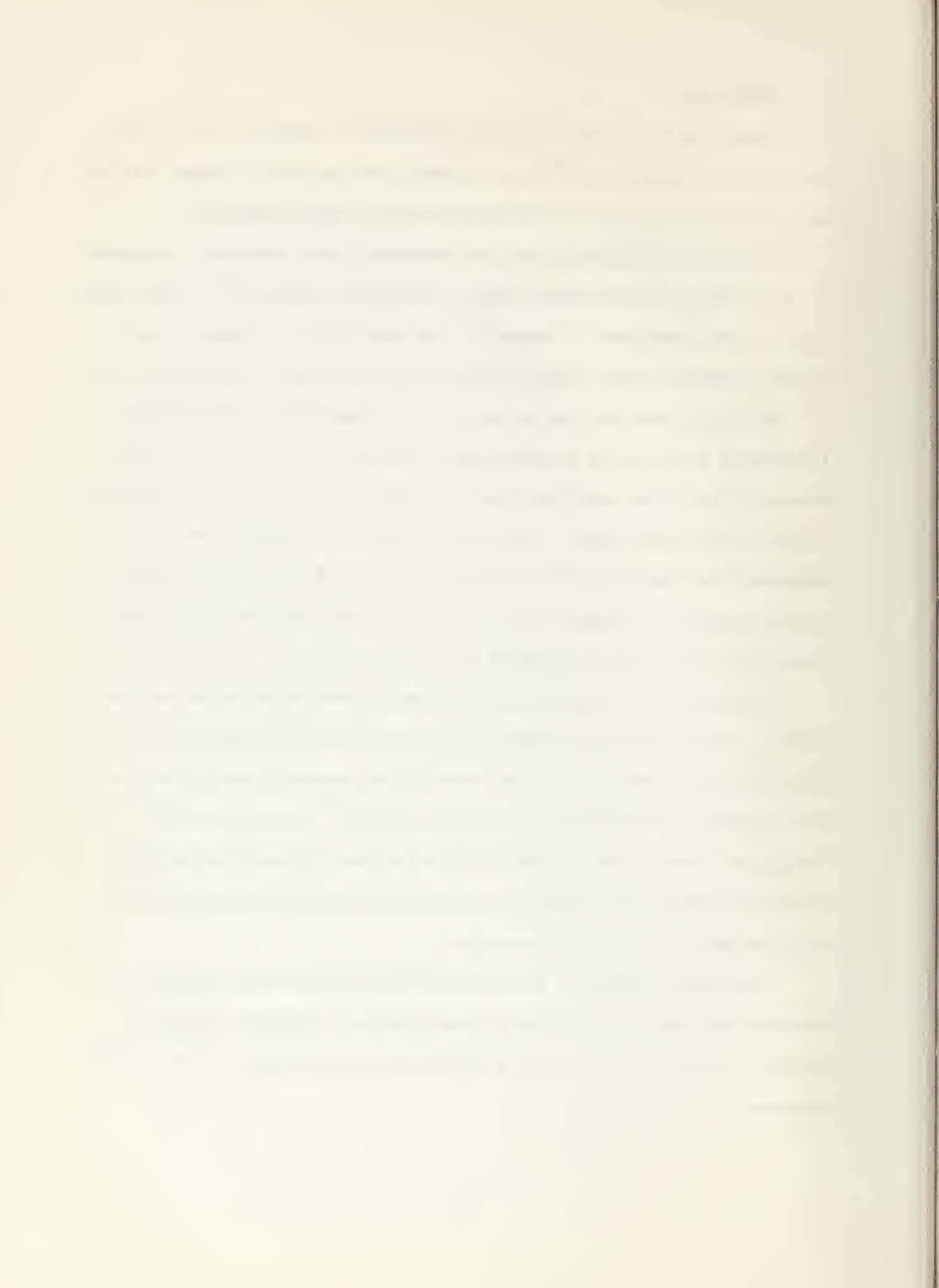
Thermal neutron absorption cross sections now reported in the literature have, in general, precisions exceeding five per cent although measurements on a few isotopes have been made to much better precisions.

One method of measuring neutron absorption cross sections is suggested by the results of first-order reactor perturbation theory [1]. This method requires the comparison of changes in the reactivity of a reactor caused by the presence of small amounts of absorbing materials of different kinds.

The AGN-201 nuclear reactor of the U. S. Naval Postgraduate School is designed for research and educational purposes. Because of the small physical size of its core, the reactor is quite sensitive to perturbations in the core configuration. The purpose of this investigation was to determine the feasibility of using the AGN-201 as a precision device for the measurement of thermal neutron absorption cross section, within the framework of first-order two-group perturbation theory.

A foil of  $\text{Au}^{197}$  was chosen as a standard absorbing material because of its large and precisely known cross section ( $98.8 \pm 0.3$  barns), the convenient half-life of its reaction product, its relative ease in handling, and its natural occurrence as one stable isotope. A foil of natural indium was chosen as an "unknown" for the purpose of investigating this technique because of its large cross section, and the relatively simple decay scheme of the reaction products.

This report presents a brief discussion of first-order two-group perturbation theory, description of experimental techniques developed, results and error analysis, and a discussion and evaluation of the methods employed.



## 2. THEORY.

First order perturbation theory yields an expression for  $\Delta \rho$ , the change in reactivity of a reactor for a small perturbation:

$$\Delta \rho = \frac{\int \phi_o^\dagger P \phi dV}{\int \phi_o^\dagger \phi dV} \quad (1)$$

where  $\phi$  is a vector representing the perturbed reactor flux,  $\phi_o^\dagger$  is a vector representing the unperturbed adjoint flux, and  $P$  is the perturbation matrix. The integral in the denominator is carried out over the volume of the reactor as a whole and that in the numerator over the volume of the perturbation. The number of energy groups determines the number of components of both vectors.

For the two-group case the vectors may be written as:

$$\phi_o^\dagger = (\phi_{o1}^\dagger \ \phi_{o2}^\dagger) \quad \text{and} \quad \phi = \begin{pmatrix} \phi_1 \\ \phi_2 \end{pmatrix}$$

where the subscripts 1 and 2 identify the fast and slow neutron groups, respectively.

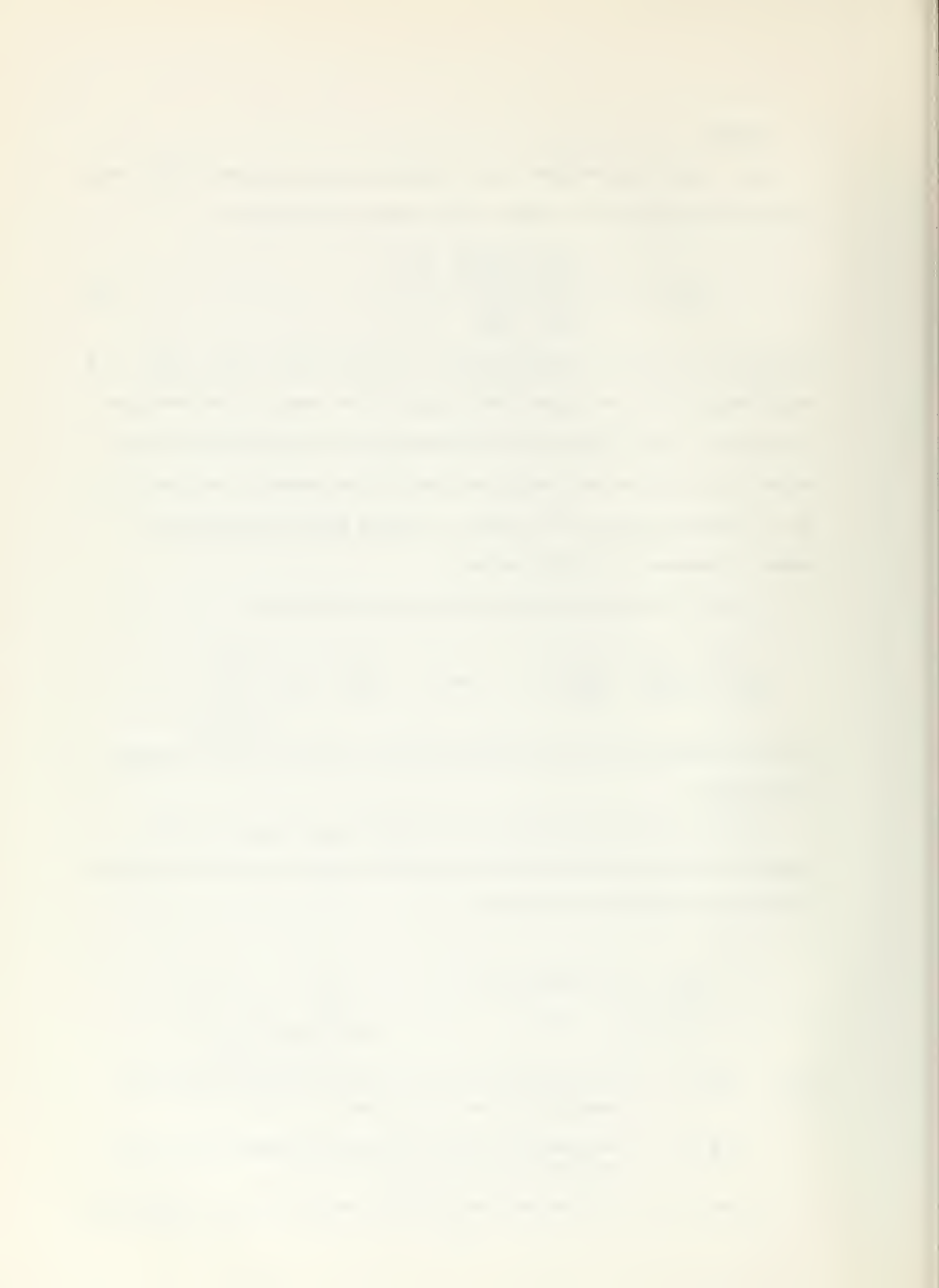
For this case and when the perturbation consists only of small changes in the absorption cross sections in a small volume of the reactor caused by the addition of a poison,

$$P = \begin{pmatrix} -(\delta \sum_{a1}) v_1 & 0 \\ 0 & -(\delta \sum_{a2}) v_2 \end{pmatrix}$$

where  $\delta \sum_{a1}$  = the change in the fast neutron average macroscopic absorption cross section and

$\delta \sum_{a2}$  = the change in the slow neutron average macroscopic absorption cross section,

$v_1$  and  $v_2$  = the average speeds of the neutron groups, respectively



Writing  $\Delta\rho = \rho - \rho_0$  where  $\rho_0$  is the reactivity with a void in the small volume, then  $\sum_{a1}$  and  $\sum_{a2}$  become  $\sum_{a1}^s$  and  $\sum_{a2}^s$ , the macroscopic cross sections of the poison itself and the expression for  $\Delta\rho$  is:

$$\rho - \rho_0 = \frac{\int (\nu_1 \phi_{o1}^+ \sum_{a1}^s \phi_1 + \nu_2 \phi_{o2}^+ \sum_{a2}^s \phi_2) dV}{\int (\phi_{o1}^+ \phi_1 + \phi_{o2}^+ \phi_2) dV} \quad (2)$$

If the effects of two poisons, identified by  $s$  and  $u$ , are being considered, the changes they produce in reactivity may be compared:

$$\frac{(\rho_s - \rho_0)}{(\rho_u - \rho_0)} = \frac{\int (\nu_1^s \phi_{o1}^{+s} \sum_{a1}^s \phi_1^s + \nu_2^s \phi_{o2}^{+s} \sum_{a2}^s \phi_2^s) dV}{\int (\nu_1^u \phi_{o1}^{+u} \sum_{a1}^u \phi_1^u + \nu_2^u \phi_{o2}^{+u} \sum_{a2}^u \phi_2^u) dV} \quad (3)$$

providing the denominator of equation (2) is essentially the same in both cases. Since the perturbation is assumed to extend over a very small

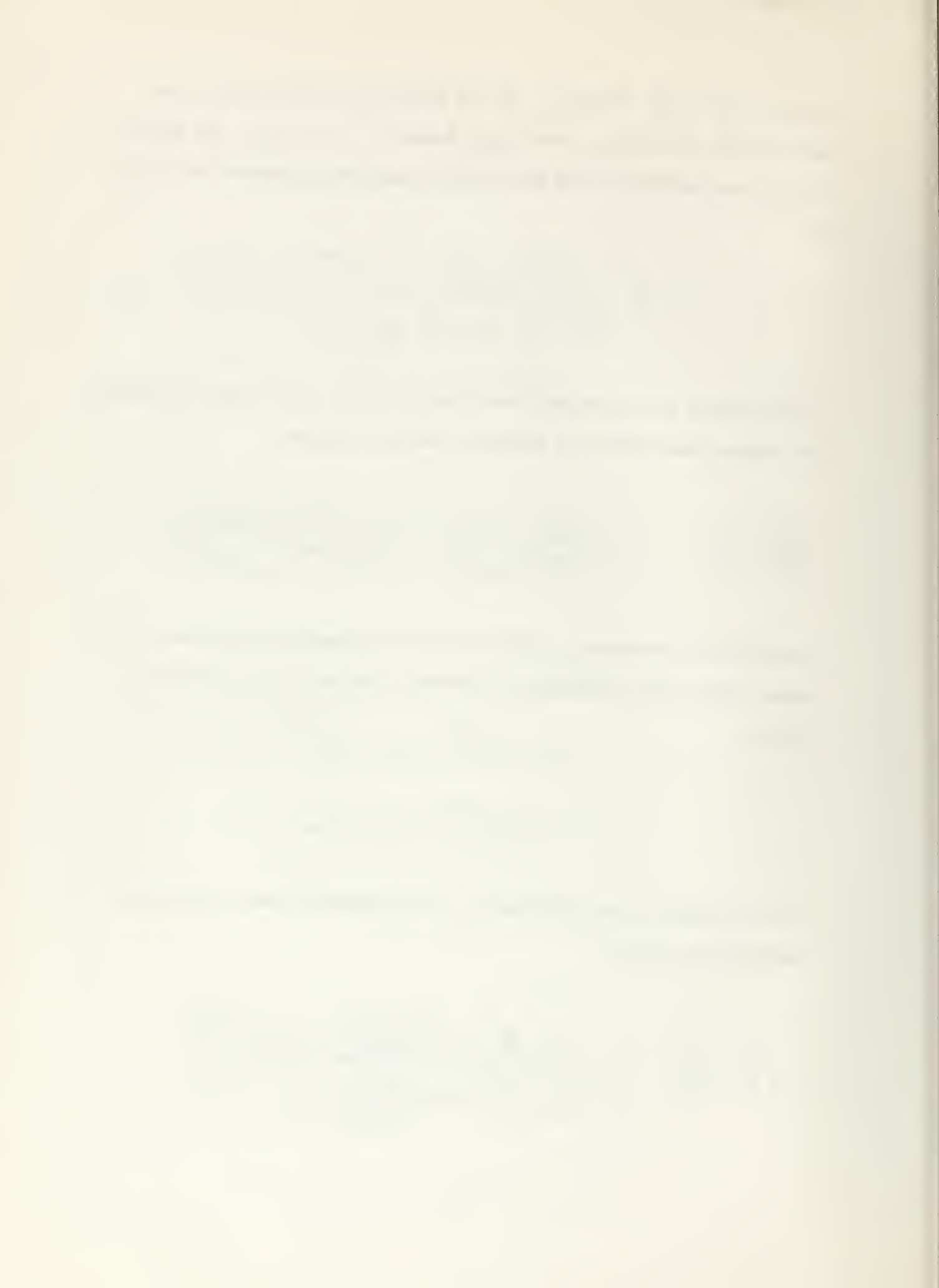
volume,

$$\nu_1^s \phi_{o1}^{+s} = \nu_1^u \phi_{o1}^{+u}$$

$$\nu_2^s \phi_{o2}^{+s} = \nu_2^u \phi_{o2}^{+u}$$

over the region of the perturbation, and equation (3) may be more conveniently written as:

$$\frac{(\rho_s - \rho_0)}{(\rho_u - \rho_0)} = \frac{\int \sum_{a2}^s \phi_2^s dV + \left\{ \frac{\nu_1 \phi_{o1}^+}{\nu_2 \phi_{o2}^+} \right\} \int \sum_{a1}^s \phi_1^s dV}{\int \sum_{a2}^u \phi_2^u dV + \left\{ \frac{\nu_1 \phi_{o1}^+}{\nu_2 \phi_{o2}^+} \right\} \int \sum_{a1}^u \phi_1^u dV} \quad (4)$$



This form lends itself to ready interpretation. The integrals represent the slow and fast absorption rates of the poisons. The quantity in curly brackets is a weighting function which expresses the relative "importance" or "worth" of fast to slow neutrons in the void with respect to overall reactor performance.

Assuming the poisons are homogeneous and defining

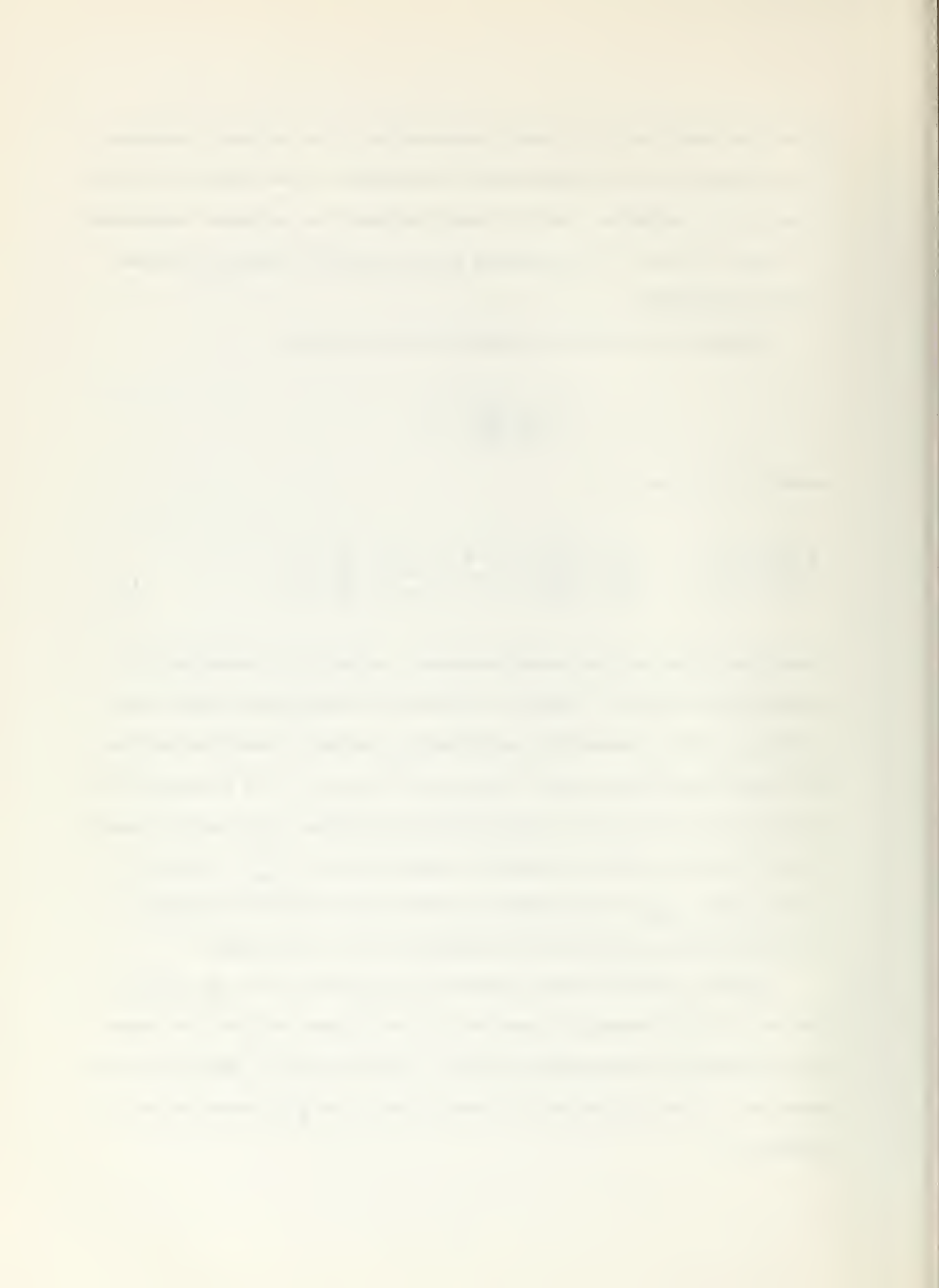
$$Y \equiv \left\{ \frac{v_1 \bar{\phi}_{o1}^f}{v_2 \bar{\phi}_{o2}^f} \right\}$$

equation (4) reduces to:

$$\frac{(\rho_s - \rho_o)}{(\rho_u - \rho_o)} = \frac{\sum_{a2}^s \bar{\phi}_2^s V^s + Y \sum_{a1}^s \bar{\phi}_1^s V^s}{\sum_{a2}^u \bar{\phi}_2^u V^u + Y \sum_{a1}^u \bar{\phi}_1^u V^u} \quad . \quad (5)$$

where the fluxes are now volume-averaged. Inspection of equation (5) shows that it relates a change in a measurable macroscopic effect (reactivity) to certain measurable microscopic processes (thermal and epithermal neutron absorption rates). Moreover, if poison "s" is a material of known cross section and "u" is a material of unknown cross section, equation (5) suggests that an analytical expression for  $\sum_{a2}^u$  may be obtained using  $\sum_{a2}^s$  as a standard, provided that Y and the necessary absorption rates and reactivity differences can be determined.

Appendix I develops from equation (5) expressions for the ratio of the fast neutron absorption rates in the two poisons and for Y in terms of experimentally observable quantities. Substitution of these back into equation (5) thus yields the following formula for  $\sum_{a2}^u$  (equation (A-2) of Appendix I):



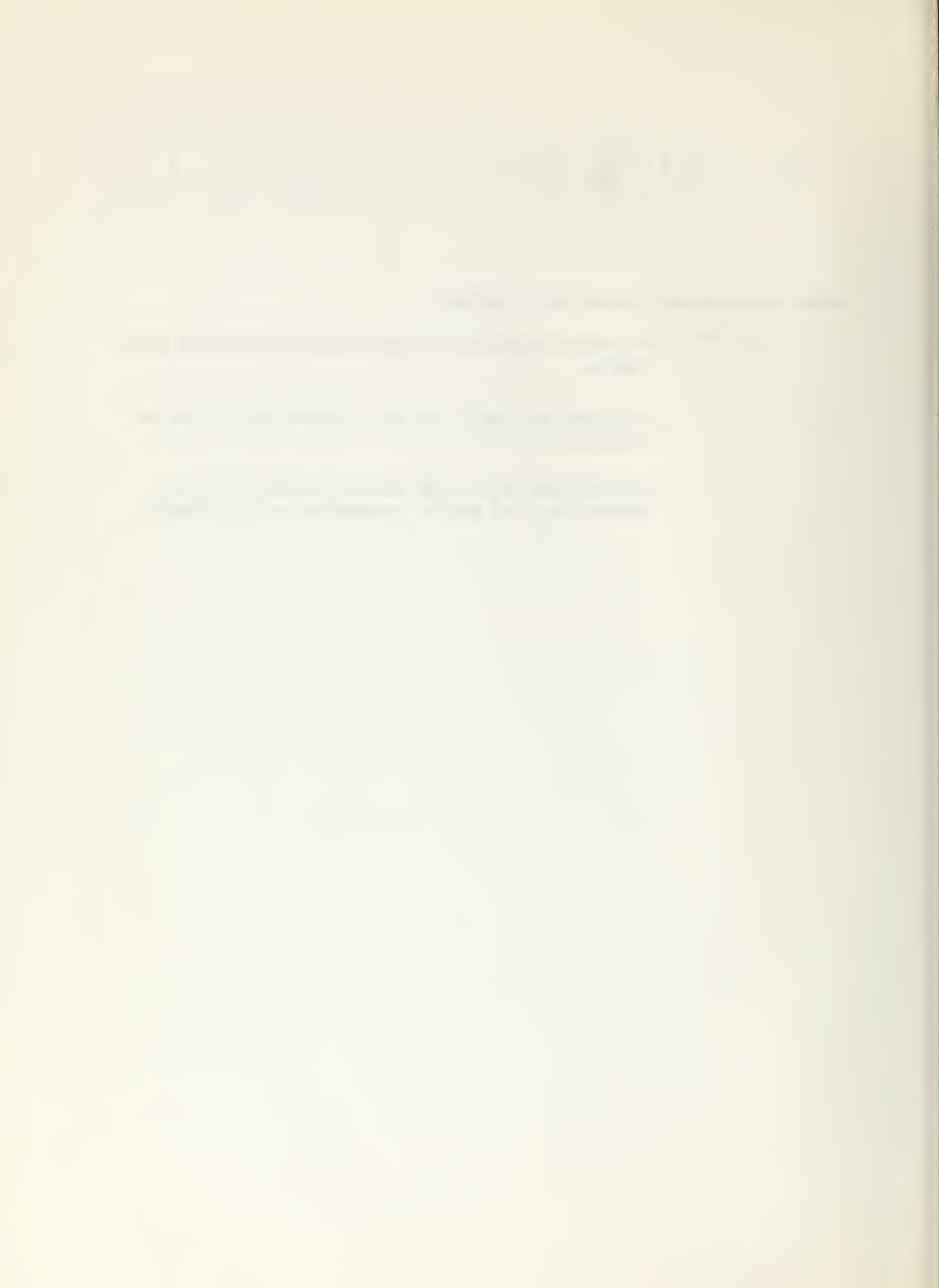
$$\sum_{\alpha_2}^u = \sum_{\alpha_2}^s \left( \frac{\bar{\phi}_2^s V^s}{\bar{\phi}_2^u V^u} \right) \left( \frac{(\rho_u - \rho_o) - \gamma^u (\rho_u^{Cd} - \rho_o^{Cd})}{(\rho_s - \rho_o) - \gamma^s (\rho_s^{Cd} - \rho_o^{Cd})} \right) \quad (6)$$

where the previously undefined terms are:

$\rho_o^{Cd}$  = the reactivity with an empty cadmium cup in the void region,

$\rho_i^{Cd}$  = the reactivity with the foil of material "i" in the cadmium cup, and

$\gamma^i$  = a correction factor / <sup>for</sup> the foil of material "i" to account for fast neutron absorption in the cadmium.



### 3. DESCRIPTION OF EXPERIMENTAL TECHNIQUES.

Inspection of equation (6) reveals that there are two basic types of measurements to be made; reactivity differences for various configurations and the ratio of the volume-averaged thermal fluxes in the standard and unknown. This section describes both the techniques developed for these measurements and the influence of geometry, temperature and instrumentation on them.

#### a) Reactivity Differences.

There are two basic methods of obtaining reactivity differences with the AGN-201 reactor.

One is from the measurement of the change in the stable period caused by the perturbation. The second is from the change in the critical position of the control rods.

Preliminary experiments indicated that stable period measurements were the most reliable, because the reactor operator found it difficult to determine when the reactor was exactly critical. Even though the initial timing for stable period measurement was accomplished using a stopwatch and observing the console linear micro-micro-ammeter, the results obtained by period measurements displayed greater reproducibility.

Having decided to use stable period measurements, it was necessary to develop reliable instrumentation for timing the rise in reactor power. Fig. 1 is a block diagram of the system devised for measuring times. In order to obtain a larger current and hence less fluctuation than in the output to the console linear micro-micro-ammeter, a  $\text{BF}_3$  ion chamber was placed in an access port of the reactor. In this position the output current was approximately 100 times greater than that provided by the reactor chamber. The signal from the ion chamber was fed to a linear



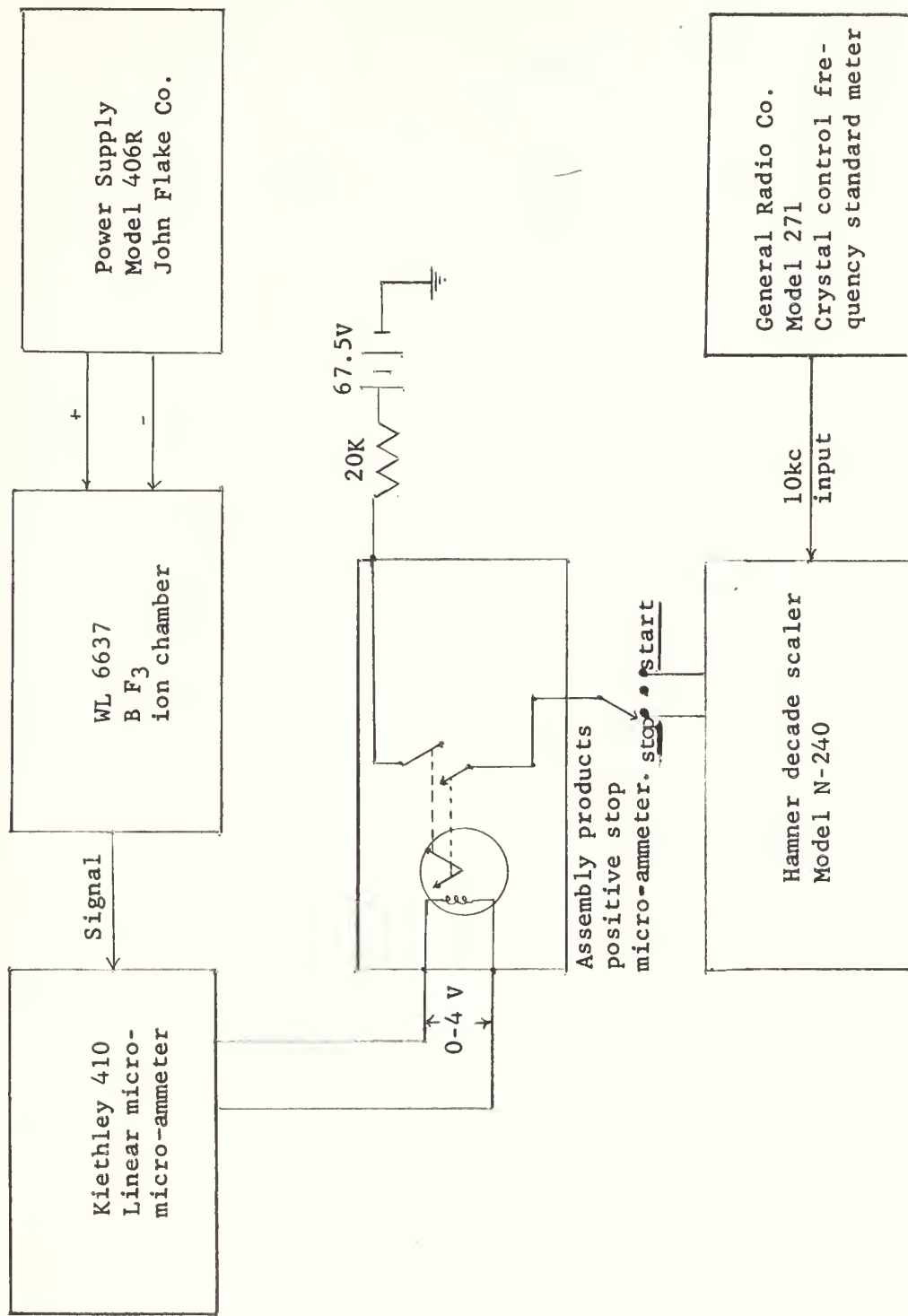


Figure 1

DIAGRAM OF THE CIRCUIT MEASURING DECADE TIME

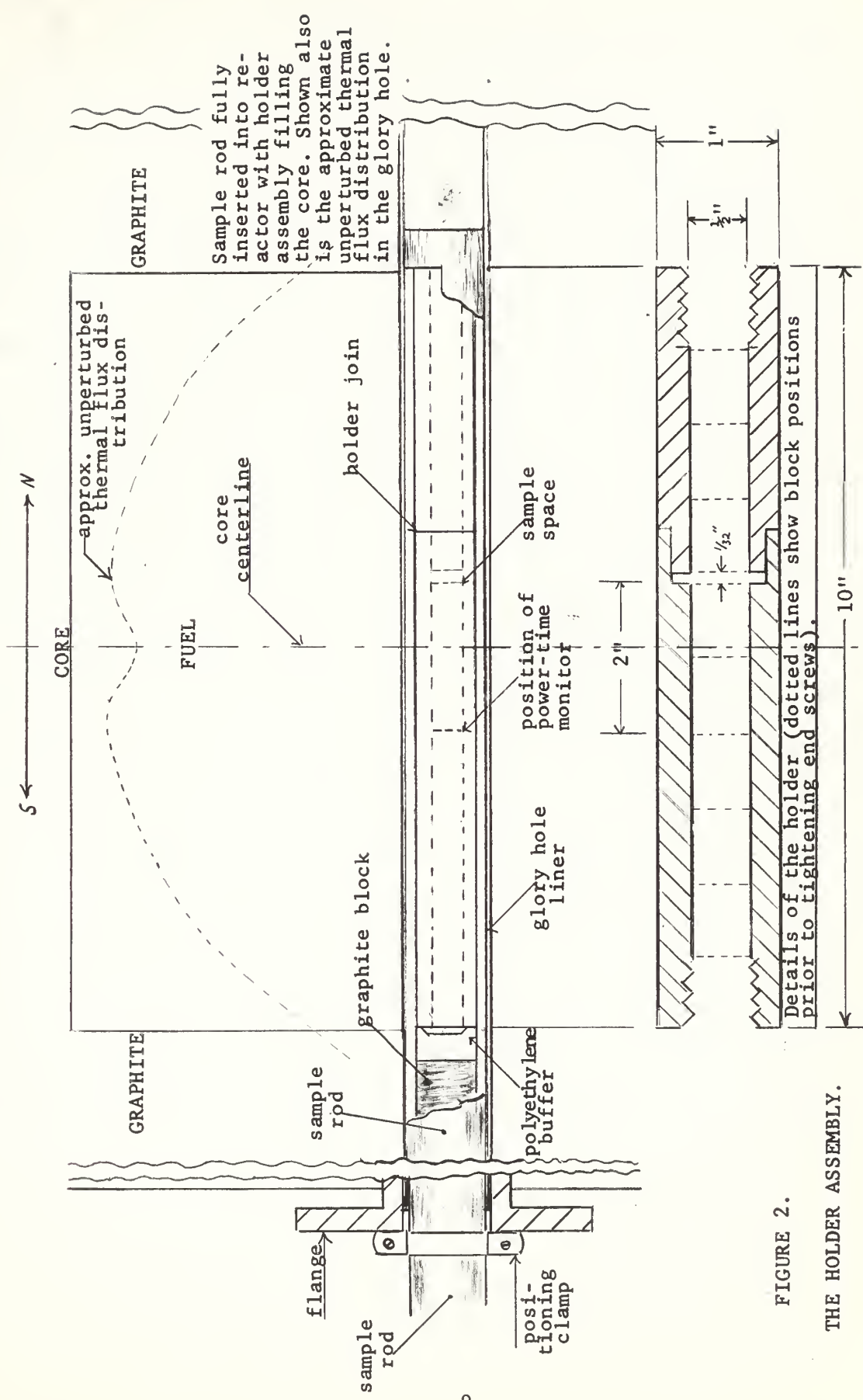


micro-micro-ammeter identical to that of the reactor console. The output of the micro-micro-ammeter was fed to a positive-stop micro-ammeter with adjustable stop. When during measurement the micro-ammeter reading first corresponded to the stop setting, the battery supplied 67.5 volts through the manual switch to start the decade scaler, which counted 10,000 cps input from the crystal-control-frequency standard meter. After the scaler was started, the scale setting on the micro-micro-ammeter was increased by a factor of ten and the manual switch moved to the "stop" position. The positive-stop meter then stopped the scaler when the power had increased by a factor of ten. This circuit was considered precise to about 5 milliseconds, the limiting component being the start-stop relay of the scaler itself, and this did not introduce any significant uncertainties into the decade time measurement. The conversion from the measured decade time to reactor period is accomplished by dividing decade time by  $\ln 10$ . The table of the inhour equation for the AGN-201 reactor of Gans [6] may be entered with the stable period to extract the reactivity.

The following techniques were used to measure the decade times for the six reactivities appearing in equation (6):

- (1) The control rods were set to hold the reactor at or near critical at approximately 10 milliwatts with the glory hole empty.
- (2) A sample rod containing the sample holder (discussed later in this section) was rapidly inserted into the south end of the glory hole (see fig. 2). Since the rod loading is largely polyethylene, the reactor would be supercritical for all perturbation configurations in the void region of the sample holder.
- (3) The power was allowed to rise by about a factor of thirty before





THE HOLDER ASSEMBLY.

FIGURE 2.



commencing decade time measurement in order that essentially all initial transients would have disappeared.

(4) After the decade time measurement had been completed, the sample rod was removed, and a special cadmium loaded "killer" rod was promptly inserted to return the reactor to 10 milliwatts.

(5) The killer rod was removed and a waiting period of six minutes observed before commencing the next measurement in order that transients would die out. The entire cycle took about fifteen minutes and the power ranges observed were from about 10 milliwatts to five watts. At no time were the control rod settings or any of the other reactor components changed. In any sequence of measurements the configurations corresponding to  $P_0$  in equation (6) were done first to determine the most reactive configuration for safety considerations. Typical periods ranged from about fifteen seconds to sixty seconds.

In order to insure that the only changes in reactor configuration from run to run occurred in the sample region, a special sample holder was devised and a clamp was used on the sample rod to insure that it was identically repositioned in the glory hole. The details of the sample holder are shown in fig. 2. The holder was 10 inches long and consisted of two mating polyethylene sleeves with inside diameter 0.525 inch in the region of the sample and 0.500 inch elsewhere. Both ends were internally threaded. Ten one-inch polyethylene plugs filled the bore. The two end ones were threaded so that they might be used to butt the plugs tightly against each other. Thus the materials in the sample region and flux monitoring foils at other positions in the holder could be held firmly and their positions reproduced by making changes in only one end of the assembly.



With half-inch diameter foils, preliminary runs made it apparent that a 10-mil thickness would be required to provide sufficiently large reactivity changes for precise determinations of the differences in reactivities with and without the sample present.

The holder in the  $\rho_o$  condition contained all materials which were required to be in the holder during flux determinations except the sample itself. (The specifications of these materials will be discussed in Section b). Briefly they are: (1) at the sample position, which is at the flux peak one inch north of core center, an incident-flux monitor foil surrounded by a gold ring, and (2) at the flux peak one inch south of core center, a power-time monitor. The  $\rho_s$  and  $\rho_u$  measurements were made with the 10-mil gold and indium foils, respectively, positioned within the gold ring and held snugly against the incident-flux monitor. The cadmium runs were made with the same loading except that in each case the gold ring with its contents was placed inside a cadmium cup 20 mils thick.

Early in the experiments on reactivity determination, it became apparent that changes in reactor temperature were affecting reproducibility of the determinations. This is not surprising since the static temperature coefficient of the reactor is large and was reported by Harvey and Ferguson [7] to be  $-0.0283\%/\text{ }^{\circ}\text{C}$ . Therefore, changes of just a few tenths of a degree could be very significant in determining reactivity of a given sample from a series of measurements. An attempt was made to measure small temperature changes in order to correct the reactivity measurement. Since the telethermometer installed on the reactor console cannot be read to less than  $0.3\text{ }^{\circ}\text{C}$ , an amplified sensitivity was required. This was obtained by use of the recorder output of the



telethermometer. By use of the circuit shown in fig. 3, small changes were recorded on the graphic recorder.

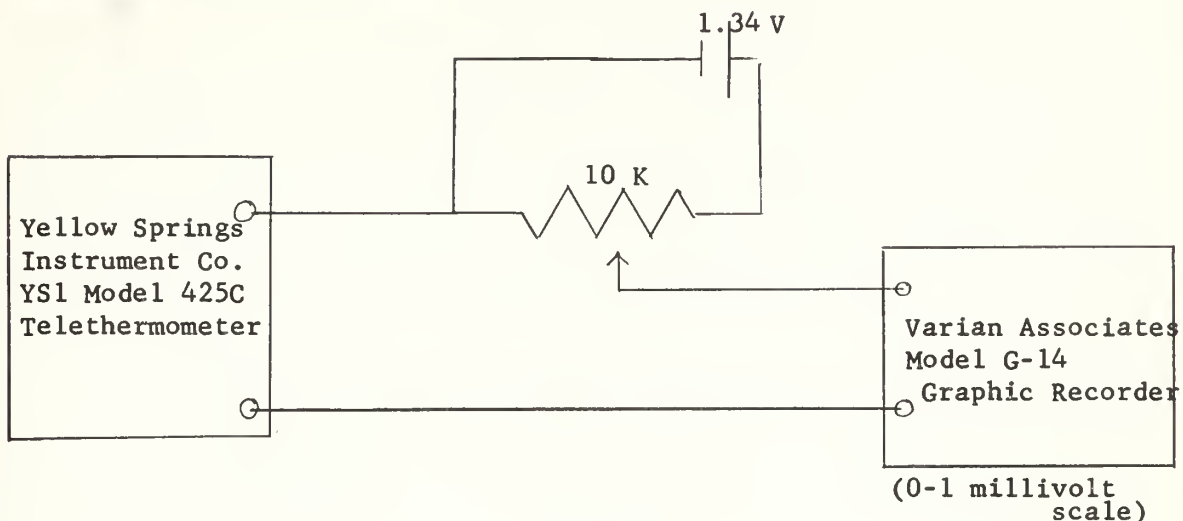


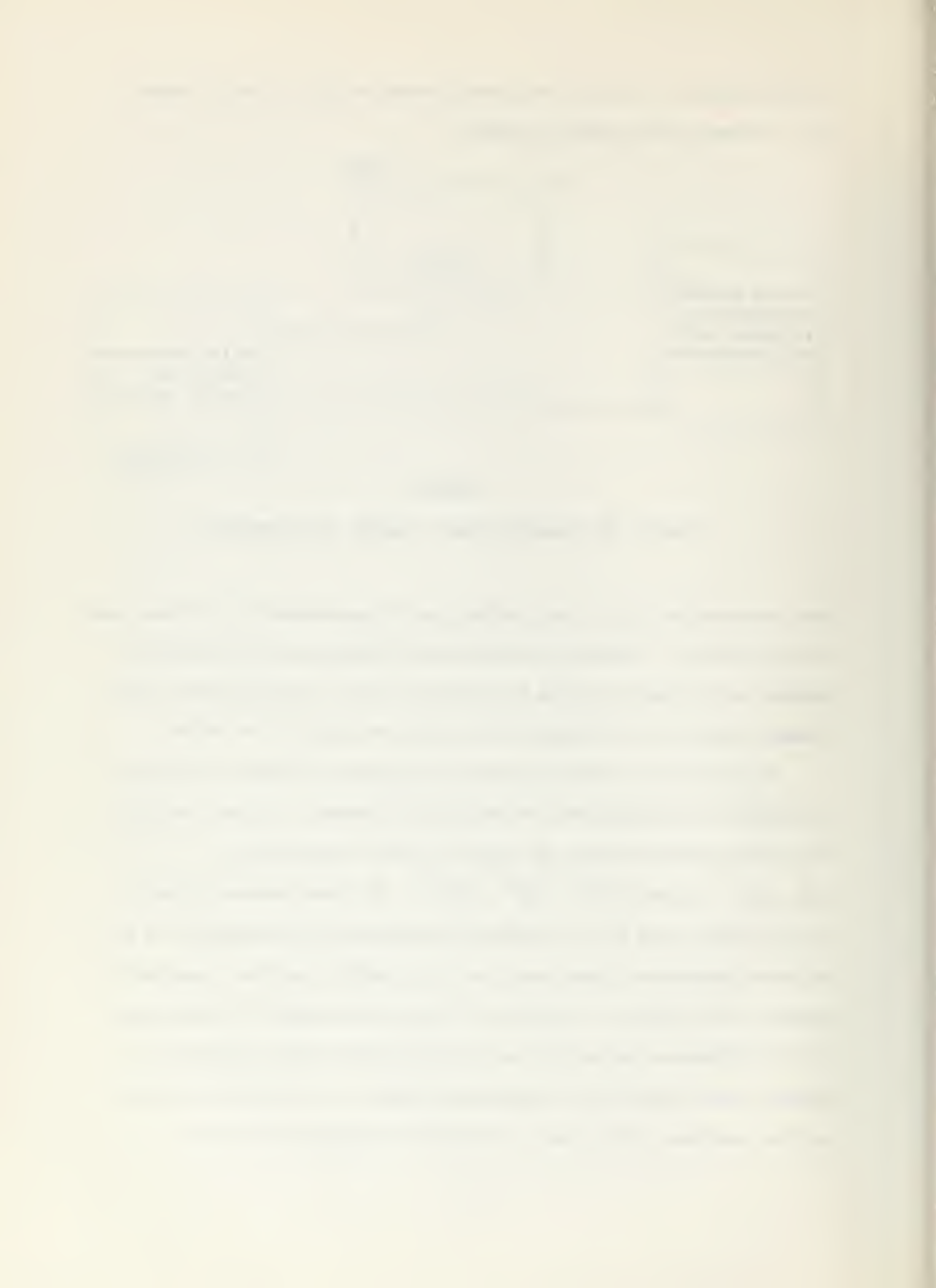
FIGURE 3

CIRCUIT FOR MEASURING SMALL CHANGES IN TEMPERATURE

This recorder had a full scale deflection of approximately  $0.7^{\circ}\text{C}$  when used in this circuit. Although it consistently indicated small temperature changes in the reactor during the reactivity runs, the magnitudes of the changes could not be determined with enough certainty to be useful.

The form of the reactivity terms in equation (6) made it possible to minimize the significance of temperature changes. The six reactivities that appear fall into two natural groups of three each:

$(\rho_u, \rho_s, \rho_o)$  and  $(\rho_u^{\text{Cd}}, \rho_s^{\text{Cd}}, \rho_o^{\text{Cd}})$ . The three members of each group are then used for two reactivity differences. Assuming that a significant temperature change would not occur within the time required to measure a full group ( $\sim$  one hour), it was then possible to obtain reactivity differences within each set of measurements with a minimum systematic error introduced by temperature changes. The precision desired in the experiment could then be obtained by repeating the sets of



measurements several times. In order to further minimize the effects of temperature, the reactor was run at five watts for about twenty minutes in an attempt to establish temperature equilibrium before beginning period measurements. In addition, the timing sequence during successive runs was carefully reproduced. These procedures gave consistent results during the final reactivity difference determinations.

b) Ratio of the Volume-averaged Thermal Fluxes.

The factor  $\frac{\bar{\phi}_2^s}{\bar{\phi}_2^u}$  in equation (6) may be obtained from the ratio of the thermal activity of the standard foil to the volume-averaged thermal flux in the unknown foil. To obtain the former, standard cadmium ratio techniques were utilized and the activities corrected for differences in radiation time and reactor power level by using the activities of a gold power-time monitor located elsewhere in the reactor;  $\bar{\phi}_2^u$  was obtained by relating the thermal activation of a thin gold "incident flux" monitor, adjacent to the unknown, to the spatial distribution of the thermal flux in the unknown, measured in a separate experiment. Activities were obtained by relative gamma counting and in all cases were extrapolated to time of removal from the reactor, corrected for dead time, background, and when necessary, self-shielding. The gold counting data were reduced using the program of Appendix II.

All counting was conducted using a 3" X 3" Harshaw NaI(Tl) scintillation detector, a type 12512 Dumont photomultiplier tube with a cathode follower, a Hamner non-overload amplifier (model N-300), a Hamner high-voltage power supply (model N-401), and a Hamner Decade Scaler (model N-240). Gamma counts were taken in the integral mode using low-voltage selection to reduce the effects of gain shift. An aluminum cap, 3" I.D. and 1/4" thick, was fitted to the scintillation detector head. A small

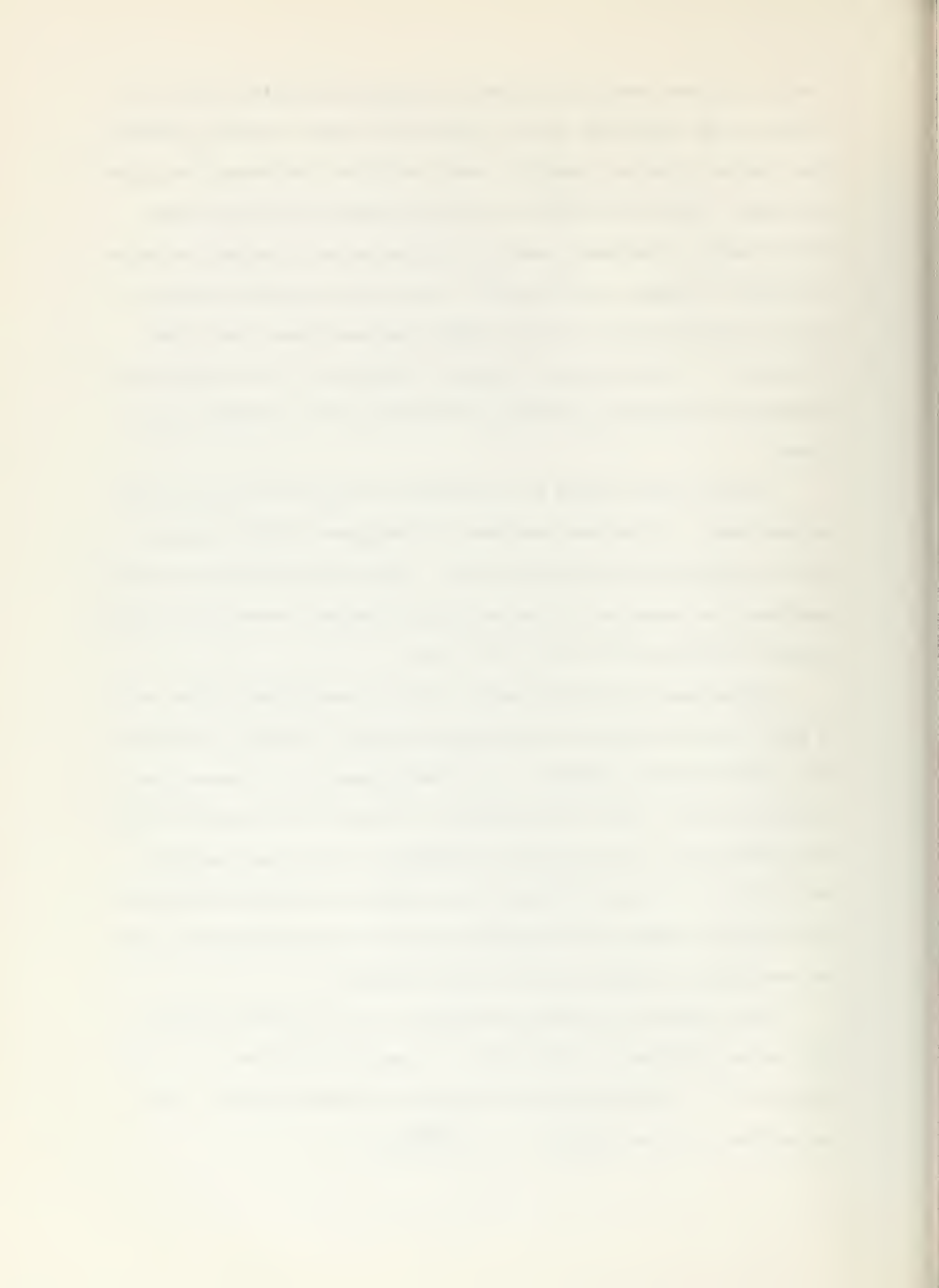


"well," 1/32 inch deep by 0.502 inch in diameter, was machined into the center of the surface of the cap; this device served a twofold purpose. The aluminum acted as a shield to avoid possible interference from beta emissions. The "well" served as a positive positioning aid for the foils counted, a necessary step since the detection efficiency is quite sensitive to change in solid angle. It was also necessary to place a 1/4-1b lead weight atop the foils while counting, because even slight curvature in an activated foil caused a difference in the counting rates obtained by turning the foil over, of the order of 3-4 standard deviations.

All foils were counted to a statistical precision of 0.1% or better on each side. Corrections were made for background, which in general was not negligible, and dead time loss. (The dead time for the counting equipment was determined by the double-pulse method, checked by an oscilloscope and found to be  $1.75 \pm .05 \mu$  sec.)

Because many of the experiments involved counting many foils over a total of several hours, precautions were taken to monitor the stability of the counting equipment. A  $C_s^{137}$  source, mounted on a copper planchette and with a count rate comparable to that of the activated foils, was counted before and after each experiment. No data were used for which the  $C_s$  count rates differed by more than two standard deviations. The counting equipment was preconditioned before measurements were made by counting an activated foil for several minutes.

Since relative  $\gamma$ -counting was employed, no corrections were made for counter efficiency, backing gain, or geometrical factors. A correction for  $\gamma$  - self-shielding was incorporated where necessary; this correction is of the form [5]:  $\epsilon = \frac{\mu \rho t}{1 - e^{-\mu \rho t}}$



where  $M$  = self shielding attenuation coefficient =  $0.19 \text{ cm}^2/\text{gm}$

$\rho$  = density of the material being counted =  $19.296 \text{ gm/cm}^3$  for rolled gold

$t$  = thickness of the material (cm)

Although the correction is small for the 0.5 mil gold foils employed, it is quite significant for the 10-mil foils. The ratio of these corrections, which will be utilized in the calculation for  $\bar{\mathcal{O}}_2^s/\bar{\mathcal{O}}_2^u$ , is  $1.045 \pm 0.001$ .

To relate  $\bar{\mathcal{O}}_2^s$  to the activities of the bare and cadmium-covered standard foil irradiated at different times, first write, for the bare case, the average count rate corrected to time of removal from reactor.

$$\dot{N}_0^s = \dot{N}^s e^{-\lambda t_w^s} = \left[ \sum_{a_2}^s \bar{\mathcal{O}}_2^s V^s + \sum_{a_1}^s \bar{\mathcal{O}}_1^s V^s \right] \left[ 1 - e^{-\lambda t_r} \right] \left[ \frac{\eta L}{E_s} \right]$$

where  $N^s$  = the average observed count rate =  $\lambda N^s / (1 - e^{-\lambda t_c})$

$N^s$  = the number of counts due to gold in time  $t_c$

$\lambda$  = decay constant of Au 198 =  $2.97462 \times 10^{-6}/\text{sec.}$

$t_w^s$  = the time from removal of the foil from the reactor to the beginning of the counting interval

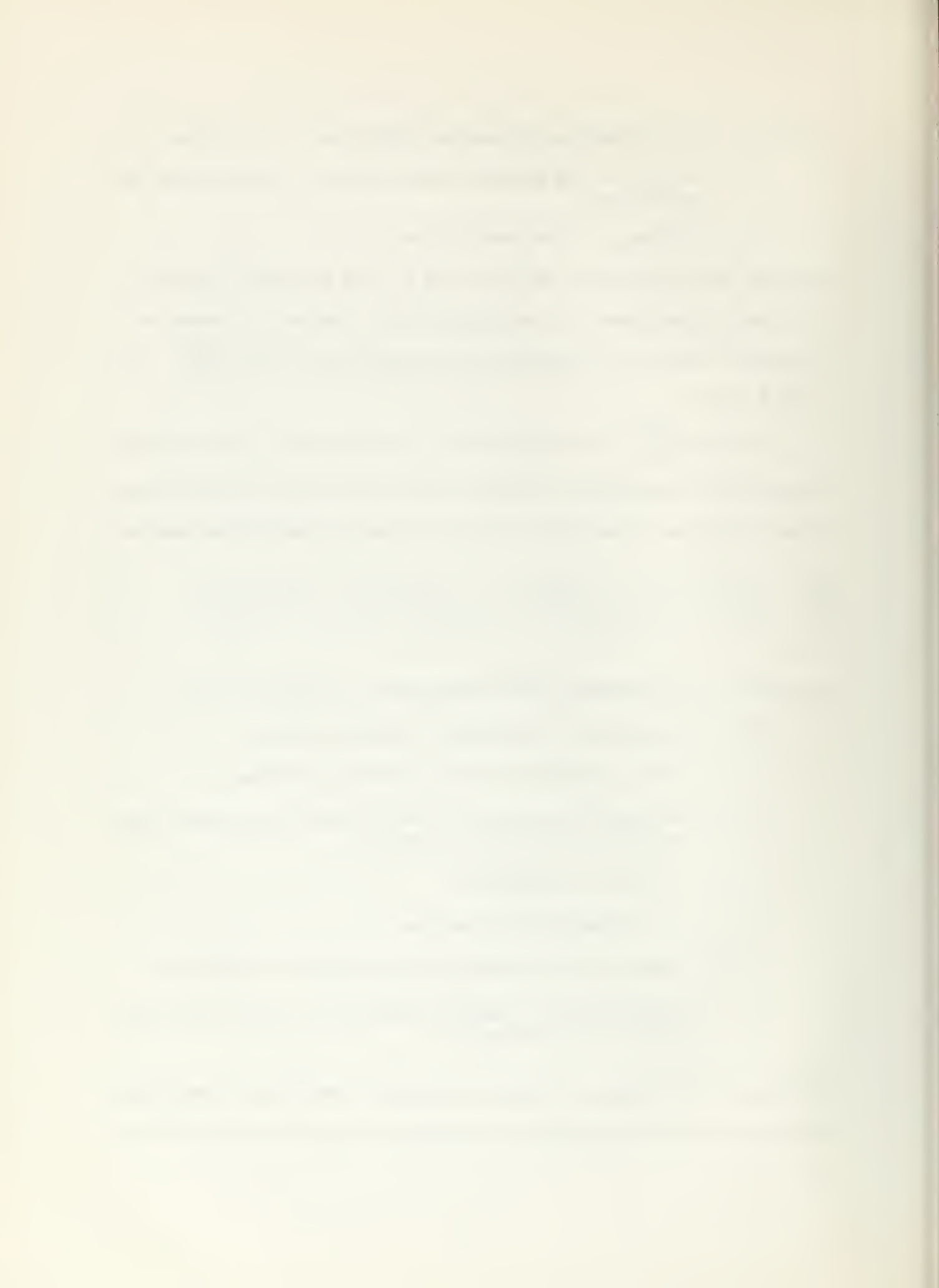
$t_r$  = the time of irradiation

$E_s$  =  $\gamma$ - self shielding correction

$\eta$  = overall counting efficiency excluding self shielding

$L$  = a dimensionless parameter accounting for the actual power level of the irradiation.

Similarly, the average count rate, corrected to the time of removal from the reactor, for the gold power-time monitor during the same irradiation is



$$\dot{P}_o = \dot{P}_e e^{-\lambda t_w} = \left[ \sum_{a2}^s \bar{\mathcal{D}}_2^p V^p + \sum_{a1}^s \bar{\mathcal{D}}_1^p V^p \right] \left[ 1 - e^{-\lambda t_r} \right] \left[ \frac{\pi L}{\epsilon_p} \right]$$

$$\text{Then } \left[ \sum_{a2}^s \bar{\mathcal{D}}_2^s + \sum_{a1}^s \bar{\mathcal{D}}_1^s \right] = \frac{\epsilon_s \dot{N}_e^s M^p}{\epsilon_p P_0 M^s} \left[ \sum_{a2}^s \bar{\mathcal{D}}_2^p + \sum_{a1}^s \bar{\mathcal{D}}_1^p \right]$$

where  $M^s$  and  $M^p$  are the masses of the standard and time-monitor foils, respectively.

Similarly, for the cadmium shielded irradiation

$$\sum_{a1}^s \bar{\mathcal{D}}_1^s = \frac{\gamma^s \epsilon_c \dot{N}_{o,cd}^s M^p}{\epsilon_p P_{o,cd} M^s} \left[ \sum_{a2}^s \bar{\mathcal{D}}_2^p + \sum_{a1}^s \bar{\mathcal{D}}_1^p \right]$$

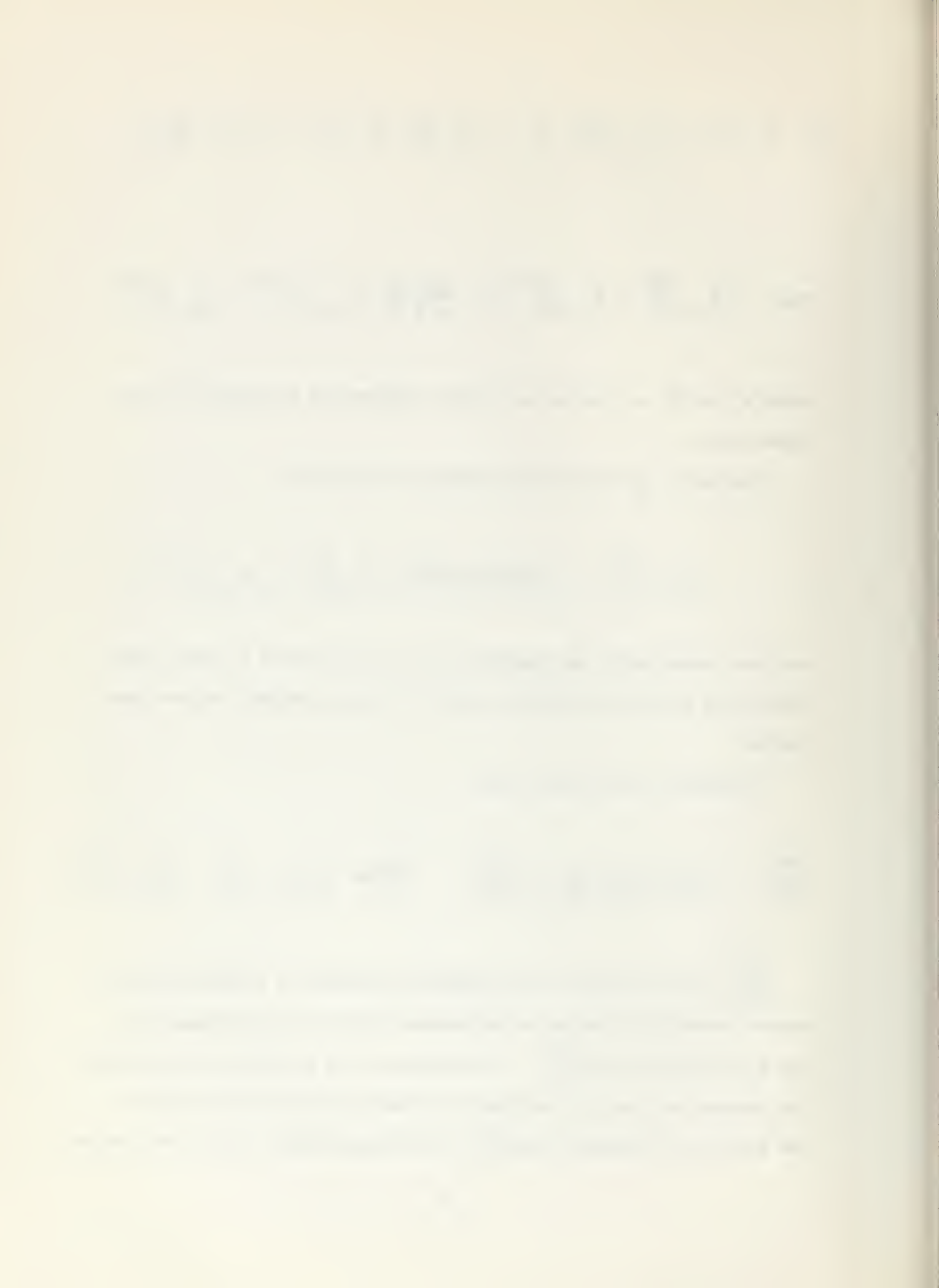
For these experiments the standard foil was enclosed in a 20-mil thick cadmium cup which was carefully sealed to prevent thermal neutron penetration.

Combining these results gives

$$\bar{\mathcal{D}}_2^s = \left( \frac{M_p}{M_s} \right) \left( \frac{\epsilon_c}{\epsilon_p} \right) \left( \frac{1}{\sum_{a2}^s} \right) \left[ \frac{\dot{N}_e^s}{P_0} - \frac{\gamma^s \dot{N}_{o,cd}^s}{P_{o,cd}} \right] \left[ \sum_{a2}^s \bar{\mathcal{D}}_2^p + \sum_{a1}^s \bar{\mathcal{D}}_1^p \right]$$

$\bar{\mathcal{D}}_2^u$  can be related to the thermal activation of a thin gold incident-flux monitor adjacent to the unknown foil in the following way.

Let  $K_1$  be the ratio of  $\bar{\mathcal{D}}_2^u$  to the thermal flux at the interface between the unknown foil and the incident-flux monitor, and  $K_2$  be the ratio of the flux at the interface and  $\bar{\mathcal{D}}_2^m$ , the average thermal flux in the monitor



itself. Then

$$\bar{\mathcal{D}}_2^u = K_1 K_2 \bar{\mathcal{D}}_2^m$$

$\bar{\mathcal{D}}_2^m$  can be determined from counting experiments in the same manner as was  $\bar{\mathcal{D}}_2^s$ . Expressed in terms of activities,  $\bar{\mathcal{D}}_2^u$  is

$$\bar{\mathcal{D}}_2^u = \left( \frac{M_p}{M_{p'm}} \right) \left( \frac{E_m}{E_p} \right) \left( \frac{1}{K_1 K_2} \right) \left[ \frac{N_e^m}{\rho'_o} - \frac{\gamma^s N_{e,cd}^m}{\rho'_{o,cd}} \right] \left[ \sum_{a2}^s \bar{\mathcal{D}}_2^{p'} + \sum_{a1}^s \bar{\mathcal{D}}_1^{p'} \right]$$

where the prime distinguishes the power-time monitor for these two irradiations from that for the standard foil.

Finally, since the two power-time monitors were essentially identical,

$$\frac{\bar{\mathcal{D}}_2^s}{\bar{\mathcal{D}}_2^u} = \left( \frac{M_p}{M_{p'm}} \right) \left( \frac{M_{p'm}}{M_s} \right) \left( \frac{1}{K_1 K_2} \right) \left( \frac{E_s}{E_m} \right) \left\{ \frac{\frac{N_e^s}{\rho'_o} - \frac{\gamma^s N_{e,cd}^s}{\rho'_{o,cd}}}{\frac{N_e^m}{\rho'_o} - \frac{\gamma^s N_{e,cd}^m}{\rho'_{o,cd}}} \right\}$$

The gold foils used were 0.500" diameter. In addition to the 10-mil gold standard three other thicknesses were employed; 2-mil gold foils served as "power-time" monitors, 0.5-mil foils were used as "incident-flux" monitors, and 1-mil foils were used in a "sandwich" technique for determining  $K_2$  as described below. Foils were cut using a light duty metal punch. Copper backing to minimize foil damage was utilized. Foil masses were determined by weighing on a Mettler type H-16 electronic balance and are precise to  $\pm 0.03$  mg. Prior to weighing, all foils were cleaned using a 50/50 dry-ether/ethanol solution.



It was felt desirable to have the sample at one of the two flux "peaks" (fig. 2) and the power-time monitor at the other. In these relatively "flat" regions of the flux profile, small imprecisions in repositioning of the sample rod would not cause an appreciable error in the relative flux "seen" by either monitors or sample.

To ascertain that the cadmium perturbation of the ambient flux would not significantly affect the power-time monitor, the following technique was adopted:

Two-mil gold foils were inserted between the blocks of the polyethylene holder assembly described earlier, one foil in each of six positions. When the entire holder assembly and sample rod were fully inserted into the "glory hole" the foil positions corresponded to one, two, three and four inches south of core center, and three and four inches north of core center. The sample position was at one inch north of core center. Two irradiations were made, the first being conducted with the cadmium cup in the sample position, and the second with the sample position empty. Construction of the sample holder guaranteed precise repositioning of the foils for the two runs.

It was expected that the ratio of specific activities of foils at corresponding positions would be identical within statistics in the regions unaffected by the cadmium, while those ratios for foils in the neighborhood of the cadmium would show a departure from the mean ratio. The ratio for the foils at the desired position of the monitor (i.e. one inch south of core center) showed no such departure, and hence was selected as an appropriate position for the power time monitor.<sup>1</sup>

---

<sup>1</sup> An interesting effect was noted during early attempts to determine these ratios. When the specific total activity ratio of two foils of



In order to determine  $K_1$  and  $K_2$ , a "sandwich" technique was utilized. A stack of thin foils (of gold for  $K_2$ ) was irradiated with the incident-flux monitor at one face. The specific thermal activation of each foil was determined, and plotted as a function of position in the stack. (The data for indium are shown in fig. 4 which appears in Section 4).

A gold ring, 5 mils thick,  $1/16"$  wide and slightly less than 0.5" in diameter was constructed (see Section 5 for details), and into this ring the "sandwich" was inserted. The purpose of the gold ring was two-fold: (1) to eliminate over-activation of the inner foils caused by small separations between their edges, and (2) to provide some physical support for the sandwich while encased in the cadmium cup during the fast neutron activation runs.

The gold sandwich consisted of, in order, the incident-flux monitor, two additional half-mil gold foils, and nine one-mil gold foils. The indium sandwich consisted of the gold incident-flux monitor and five two-mil indium foils.

$K_1$  was obtained from the graph of fig. 4 and the computed total specific activities of indium.  $\alpha_{th}(\text{incident})$ , which is directly proportional to the thermal flux at the interface between the indium foils and the incident flux monitor, was obtained by extrapolation of the data points.

---

considerably different masses was compared with that of two foils of nearly the same mass, the heavier foil was "colder" than the lighter foil. In the cases noted, the two foils differed in mass by about 10%. The apparent difference in specific activity was approximately 1%. This anomaly is probably due to the difference in behavior of the epithermal and thermal flux through the volume of the foil. An approximate calculation of the relative flux depression and their effect on specific



$K_2$  was obtained from a similar plot of the gold data.

The gold ring and the incident flux monitor thus become an integral part of the holder assembly for all reactivity and flux measurements.

---

activity through two gold foils, differing in thickness by 10%, using the known thermal cross-section and effective resonance integral of gold, substantiates this explanation. Therefore, the foils used in all subsequent traverse experiments and as power-time monitors had masses matched to within 0.25 mg.



#### 4. RESULTS AND ERROR ANALYSIS.

##### a) Reactivity Measurements.

The results of the reactivity measurements are expressed first in terms of the four reactivity differences of equation (6); these are then combined with the cadmium correction factors to yield the overall result:

$$D = \frac{(\rho_u - \rho_o) - \gamma^u (\rho_u^{Cd} - \rho_o^{Cd})}{(\rho_s - \rho_o) - \gamma^s (\rho_s^{Cd} - \rho_o^{Cd})}$$

Six measurements were made of the set  $(\rho_u, \rho_s, \rho_o)$  and three of the set  $(\rho_u^{Cd}, \rho_s^{Cd}, \rho_o^{Cd})$ . The means of the four reactivity differences and their variances were calculated assuming the differences were normally distributed. It is noted that by treating each reactivity difference as a random variable, no allowance was made for the fact that  $\rho_o$  and  $\rho_o^{Cd}$  each appear in two terms. This introduces a correlation in the estimated variances. Because of the form of  $D$ , the estimated variances will be larger than the true ones.

The values of the cadmium correction factors are taken from reference [3]. Their standard deviations are estimated. Column 1 of Table 1 lists these results and their estimated standard deviations. Reactivity differences are expressed in per cent. Column 2 shows the contribution of each term to the variance of  $D$  which was calculated using Gaussian error propagation.



TABLE I  
RESULTS OF REACTIVITY MEASUREMENTS

	Column 1	Column 2
		( $\times 10^6$ )
$\rho_u - \rho_o$	$0.02571 \pm 0.00012$	47
$\rho_s - \rho_o$	$0.02018 \pm 0.00014$	88
$\rho_u^{Cd} - \rho_o^{Cd}$	$0.00395 \pm 0.00007$	19
$\rho_s^{Cd} - \rho_o^{Cd}$	$0.00267 \pm 0.00002$	1
$\gamma^s$	1.015 $\pm .005$	3
$\gamma^u$	1.095 $\pm .005$	5
D	1.224 $\pm .013$	<hr/> 163



b) Ratio of the Volume-averaged Thermal Fluxes.

Difficulty was experienced in obtaining reproducible results for the sandwich experiments; this is discussed at length in Section 4. The results from the most reliable data were used to calculate  $K_1$  and  $K_2$ . Fig. 4 is a plot of the data for  $K_1$ . The estimated precision in the specific activities, which included counting statistics and the uncertainties due to mass measurements only, were about 0.10%. The estimated precisions of  $K_1$  and  $K_2$  include uncertainties due to the graphical analyses used and to other random effects intrinsic to the sandwich technique. The values are:

$$K_1 = 0.9890 \pm 0.0054$$

$$K_2 = 0.9816 \pm 0.0014$$

The counting rates for the standard foil and the incident flux monitor are precise to approximately 0.1%. Foil mass measurements were known to about 0.03 mg. Combining the uncertainties in all factors gives

$$\frac{\bar{\phi}_s}{\bar{\phi}_u} = 1.0610 \pm 0.0060$$

The precision is dominated by the uncertainties in  $K_1$  and  $K_2$ .

c) The 2,200 m/sec Microscopic Cross Section of Indium.

Equation (6) may be rewritten in terms of the microscopic neutron absorption cross sections of the standard and unknown materials averaged over the thermal neutron spectrum of the AGN-201 reactor at 20.0°C.



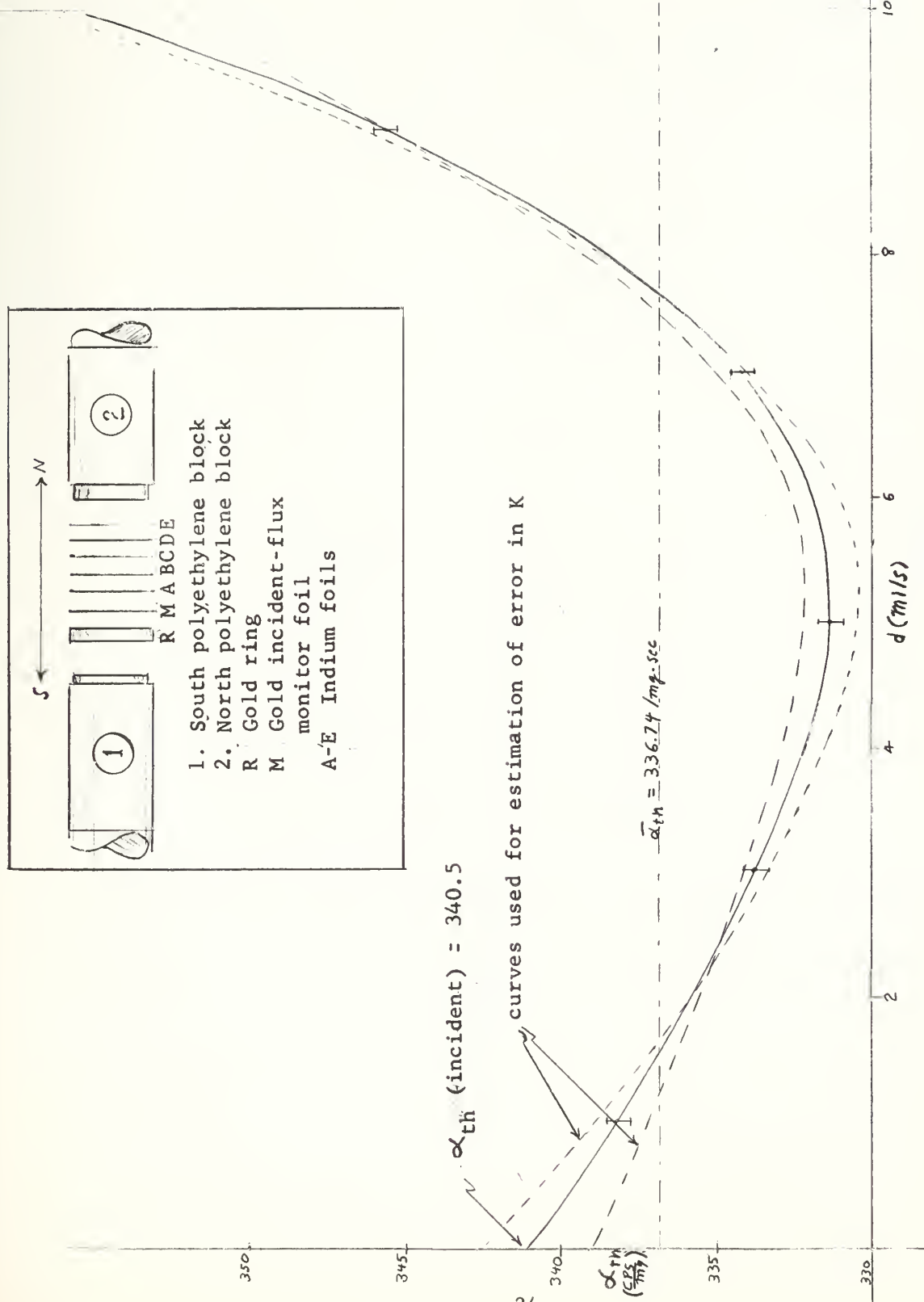


Figure 4.

SPECIFIC THERMAL ACTIVITY WITHIN INDIUM FOIL

The specific thermal activity ( $\alpha_{th}$ ) in a ten-mil indium foil is plotted as a function of distance ( $d$ ) from the interface between the indium and an incident-flux monitor. An insert shows details of the sandwich assembly.



$$\bar{\sigma}_{a2}^u = \bar{\sigma}_{a2}^s \left\{ \frac{M_s}{M_u} \right\} \left\{ \frac{W_u}{W_s} \right\} \left\{ \frac{\bar{\sigma}_s^s}{\bar{\sigma}_s^u} \right\} \left\{ D \right\} \sqrt{\frac{293.0}{T}}$$

where  $W_s$  and  $W_u$  are the atomic weights of the standard and unknown materials, respectively, and  $T$  is the absolute temperature of the reactor during the experiments. The results for the factors in this expression and the estimates of their standard deviations are:

$\bar{\sigma}_{a2}^s$	$98.8 \pm 0.3$ barns	[4]
$M_s$	$614.34 \pm 0.05$	
$M_u$	$234.16 \pm 0.05$ mg	
$W_u$	114.82	[8]
$W_s$	197.0	[8]
$\bar{\sigma}_s^s / \bar{\sigma}_s^u$	$1.0610 \pm .0060$	
$D$	$1.224 \pm .013$	
$T$	$294.5 \pm 0.3$ °K	

Combining these quantities gives

$$\bar{\sigma}_{a2}^u = 194.4 \pm 2.3 \text{ barns.}$$

Assuming that the energy dependences of the gold and indium cross sections in the thermal range are not significantly different,  $\bar{\sigma}_{a2}^u$  may be compared to  $196 \pm 5$ , the published 0.0253-ev value of the cross section for indium [4].



## 5. DISCUSSION AND CONCLUSIONS.

The result obtained for the cross section of indium is of considerably better precision than that reported in current literature providing no hidden systematic error is present. It is apparent, however, that even more precise determinations are possible with further refinement of these techniques. The two measurements that limit the precision of the determination in this experiment are bare reactivity differences and the flux depression factor  $K_1 K_2$  which relates the average flux in the incident flux monitor to the average flux through the sample foil.

The determination of reactivities may prove quite difficult to improve. Although the AGN-201 is well suited to measurements of reactivity changes caused by samples of small physical size, it is also very sensitive to temperature changes which may be caused by a change in environmental conditions as well as internal changes. A considerable number of trials were conducted in order to determine how to achieve maximum temperature stability and how to measure small temperature changes. Although a technique was developed to minimize the effects of temperature change, no positive means of measuring these changes was achieved.

One method of further minimizing the temperature effect would be to take sets of measurements consisting of only the two reactivities occurring in each of the reactivity differences. This would require determination of  $\rho_o$  and  $\rho_o^{Cd}$  each time a difference in which they are used is measured.

The method which, if accomplished, would provide much better control over the experiment would be the design of a device capable of precise detection of small temperature changes and a careful measurement of the dynamic temperature coefficient of reactivity at low powers. The



sensor for such a device must be investigated, however, as apparent temperature changes of small magnitude as observed on the specially designed temperature recorder detected by the sensor of the telethermometer were not accompanied by the immediate reactivity effects expected with this change; usually the reactivity effects were observed at some later time. Furthermore, use of the static temperature coefficient of Harvey and Ferguson did not give consistent correlations.

A possible source of systematic error was present in the reactivity determinations because the foils were subjected to bending and warpage when being fitted inside the gold ring. The fact that the sample was changed for each successive run increased the opportunity for such damage to occur. Foil handling could be reduced to a minimum if proper temperature corrections could be made, thus allowing repeated measurements of the same configuration.

As with reactivity measurements, the sandwich technique used for determination of average thermal flux in the unknown could be considerably improved.

Several early experiments were devoted to application of this method to a gold sandwich of the same size, but composed of nine 1-mil gold foils in the sandwich body with two half-mil foils at the surface adjacent to the half-mil monitor. In all instances save one, however, the technique failed; the cadmium-shielded irradiations produced anomalously high activities among the lighter foils, leading directly to an apparent thermal depression at these positions. This was probably caused by some separation of these small foils from the body of the sandwich during the cadmium irradiation. The single success involved a sandwich composed of four two-mil, one one-mil, and three half-mil foils (this series



is that from which  $K_2$  was computed).

To fully appreciate the origins of this condition, it is necessary to review the details of preparing the sandwich-ring assembly. The sandwich is contained by a 5-mil X 1/16" gold ring, of slightly smaller diameter than that of the sandwich itself. This ring is fabricated in the following manner: a strip of gold about 1/16" wide is cut from a sheet of 5-mil stock in the shape of an elongated cross, the arms of which have a span of about 3/16". The head of the cross is beaten down to a thin taper and trimmed to the width of the cross body. The strip is then rolled around a polyethylene cylinder which has previously been cut down at the end by about two mils from an original .500" diameter. The body of the cross is pulled back tightly across the tapered head, the arms fold up and over and are then pressed down, locking the assembly in the shape of a ring. Extra material is trimmed away. The ring may be then carefully worked up the cylinder until it is held by only about 1/4 its thickness. Foils may be inserted at this time, pressing them down with undercut polyethylene blocks so that the edges of the foils bind tightly against the sides of the ring. If accomplished with great care, the whole assembly may be lifted free of the matrix and inserted in its cadmium shield. The same loading procedure is followed after the cadmium irradiation is completed and counted.

This cadmium irradiation is the most difficult phase. While within the cadmium cup, the foils have no positive agent pressing them tightly together. Instead, the foils are supported only by the pressure of their edges against the sides of the ring. It is apparent that error in loading technique might allow a poor purchase, especially among the thin foils, allowing the crucial thinner foils to work loose during irradiation.



"Hyperactivation" would result. The fact that this effect was not noted on the single successful run may be attributed to the fact that two-mil foils were utilized in the body of the sandwich during this experiment, rather than one mil. These heavier foils may have allowed a more uniform loading, and the additional stiffness behind the outer monitors may have prevented their working loose during irradiation.

The indium sandwiches suffered from their own problems peculiar to the nature of the material. Because indium tends to be somewhat adherent, no trouble was experienced because of separation of the foils in the sandwich. However, because indium is also extremely soft, foil damage was most difficult to avoid, especially in the form of weight loss (at the edges) during loading. This necessitated reweighing the foils after each irradiation.

Edge damage, not only to indium, but to gold also, may have contributed to the poor results; it is almost certain that some foils were somewhat marred about the circumference during one of the loadings.

The fact that the gold ring could conceivably slip relative to the sandwich proper, allowing one face to be more in the neutrons' "shadow" of the protruding gold cylinder than the other, might have introduced error. Pains were taken to prevent such an occurrence by machine tooling the blocks and by careful visual inspection of the sandwich before and after each irradiation.

In summary, it is felt that this method of flux depression measurement is feasible in principle, but that a significant improvement in both precision and reliability could be achieved by the development of a better mechanical scheme for loading and holding the foils in the sandwich.



In conclusion, the authors believe that the feasibility of the methods developed for cross section measurements has been demonstrated and that, although the reported results reflect a considerable improvement on other methods of thermal cross section measurement for certain isotopes, the precision of 1.2% attained in this investigation can be bettered with a minimum of further experimentation.



## 6. ACKNOWLEDGEMENTS.

The authors wish to express appreciation to the many people who provided assistance to the success of this experiment. These include: Professors J. W. Schultz, G. H. Spencer, and W. M. Tolles of the Department of Material Science and Chemistry, for assistance in the precise weight determinations; Professors F. Bumiller and E. A. Milne of the Department of Physics for providing materials which greatly assisted in this investigation; to Mr. H. L. McFarland for the many extra hours he gave in his skillful operation of the reactor and for his assistance in the electronics problems in the design of measuring systems; and most especially to Professor Harry E. Handler for his instruction, assistance and encouragement throughout the entire project.



#### BIBLIOGRAPHY

1. Glasstone, S. and M. C. Edlund. The Elements of Nuclear Reactor Theory. D. Van Nostrand Co., 1952.
2. Hughes, D. J. Pile Neutron Research. Addison-Wesley Co., 1953.
3. Martin, D. H. Correction Factors for Cd-Covered-Foil Measurements, Nucleonics, v. 13. March, 1955: 52-53.
4. Hughes, D. J. Neutron Cross Sections, BNL 325. Brookhaven National Laboratory, 1958, 2d ed.
5. Sola, A. Flux Perturbation by Detector Foils. Nucleonics, v. 18. March, 1960: 78-81, 141.
6. Gans, G. M., Jr. Design of an Automatic Flux Level Control System for the AGN-201 Reactor. Master's Thesis, United States Naval Post-graduate School, Monterey, California, 1963.
7. Ferguson, D. E. and W. D. Harvey. Determination of AGN-201 Reactor Operating Parameters at High Powers. Master's Thesis, United States Naval Postgraduate School, Monterey, California, 1963.
8. Chemical Rubber Company. Handbook of Physics and Chemistry, v. 45, 1963.



## APPENDIX I

### EXPRESSION OF EQUATION (6) IN TERMS OF EXPERIMENTALLY OBSERVABLE PARAMETERS

Suitable algebraic manipulation permits (6) to be solved explicitly

for  $\sum_{a2}^u$  :

$$\sum_{a2}^u = \sum_{a2}^s \left( \frac{\rho_u - \rho_o}{\rho_s - \rho_o} \right) \left( \frac{\bar{\phi}_2^s v^s}{\bar{\phi}_2^u v^u} \right) \left[ 1 + Y \frac{\sum_{a1}^s \bar{\phi}_1^s v^s}{\sum_{a2} \bar{\phi}_2^s v^s} \left\{ 1 - \frac{\rho_s - \rho_o}{\rho_u - \rho_o} \left( \frac{\sum_{a1}^u \bar{\phi}_1^u v^u}{\sum_{a1} \bar{\phi}_1^s v^s} \right) \right\} \right] \quad (A-1)$$

Besides the reactivity differences,  $(\rho_u - \rho_o)$  and  $(\rho_s - \rho_o)$ , and the ratio of the volume-averaged thermal fluxes in the two materials, the quantities which must be measured are the ratio of the fast neutron absorption rates in the unknown and standard materials, the ratio of the fast to slow neutron absorption rates in the standard material, and the relative worth of fast and slow neutrons (Y).

$$\frac{\sum_{a1}^u \bar{\phi}_1^u v^u}{\sum_{a1}^s \bar{\phi}_1^s v^s}$$

The ratio of the fast neutron absorption rates can be obtained by using cadmium cups to filter out the thermal neutrons. If the void reactivity of equation (5) refers to a void inside a cadmium cup, equation (5) becomes:

$$\frac{\rho_u^{Cd} - \rho_o^{Cd}}{\rho_s^{Cd} - \rho_o^{Cd}} = \frac{\sum_{a1}^u \bar{\phi}_1^u v^u \gamma^s}{\sum_{a1}^s \bar{\phi}_1^s v^s \gamma^u}$$

Where:

$\rho_u^{Cd}$  = Reactivity observed for cadmium-shielded unknown material

$\rho_s^{Cd}$  = Reactivity observed for cadmium-shielded standard material



$\rho_o^{Cd}$  = Reactivity observed for the empty cadmium shielding.

Then the ratio  $\frac{\sum_{al}^u \overline{\phi}_1^u v^u}{\sum_{al}^s \overline{\phi}_1^s v}$  may be

written as  $\frac{\gamma^u}{\gamma^s} \left( \frac{\rho_u^{Cd} - \rho_o^{Cd}}{\rho_s^{Cd} - \rho_o^{Cd}} \right)$ .

$$Y = \frac{v_1 \overline{\phi}_1^{\dagger}}{v_2 \overline{\phi}_2^{\dagger}}$$

Substituting the cadmium-covered standard material for the unknown in equation (5)<sup>1</sup>:

$$\frac{\rho_s - \rho_o}{\rho_s^{Cd} - \rho_o} = \frac{\sum_{a2}^s \overline{\phi}_2^s v^s + Y \sum_{al}^s \overline{\phi}_1^s v^s}{\sum_{a2}^{Cd} \overline{\phi}_2^{Cd} v^{Cd} + Y \sum_{al}^{Cd} \overline{\phi}_1^{Cd} v^{Cd} + Y \sum_{al}^s \overline{\phi}_1^s v^s \frac{1}{\gamma^s}}$$

Similarly, substituting the empty cadmium cup for the unknown in equation (5)<sup>1</sup>:

$$\frac{\rho_s - \rho_o}{\rho_o^{Cd} - \rho_o} = \frac{\sum_{a2}^s \overline{\phi}_2^s v^s + Y \sum_{al}^s \overline{\phi}_1^s v^s}{\sum_{a2}^{Cd} \overline{\phi}_2^{Cd} v^{Cd} + Y \sum_{al}^{Cd} \overline{\phi}_1^{Cd} v^{Cd}}$$

<sup>1</sup>The validity of this expression depends upon the approximate equality of the quantity  $\int (\overline{\phi}_{o1}^{\dagger} \overline{\phi}_1 + \overline{\phi}_{o2}^{\dagger} \overline{\phi}_2) dV$  with the cadmium cup in or out of the reactor. A rough calculation utilizing the known spatial dependence of the flux for the two cases indicated that the percentage difference is about 0.13% which is smaller than other errors in the determination of Y.



Note that  $\bar{\phi}_1^{Cd*}$  differs from  $\bar{\phi}_1^{Cd}$  because the epithermal flux in the cadmium is affected by the presence of the standard material.

Inverting these two expressions, subtracting and solving for  $Y$  gives:

$$Y = \frac{\sum_{a2}^s \bar{\phi}_2^s}{\sum_{a1}^s \bar{\phi}_1^s} \left[ \frac{\gamma^s \left( \frac{p_s^{Cd} - p_o^{Cd}}{p_s - p_o} \right)}{1 - \gamma^s \left( \frac{p_s^{Cd} - p_o^{Cd}}{p_s - p_o} \right) + \frac{\gamma^s \left[ \sum_{a1}^{Cd} \bar{\phi}_1^{Cd} V_1^{Cd} - \sum_{a1}^{Cd*} \bar{\phi}_1^{Cd*} V_1^{Cd} \right]}{\sum_{a1}^s \bar{\phi}_1^s V_1^s}} \right]$$

Rewriting the third term in the denominator as:

$$\frac{\gamma^s \sum_{a1}^{Cd} V_1^{Cd}}{\sum_{a1}^s V_1^s} \left[ \frac{\bar{\phi}_1^{Cd} - \bar{\phi}_1^{Cd*}}{\bar{\phi}_1^s} \right]$$

and approximating  $\frac{\bar{\phi}_1^{Cd}}{\bar{\phi}_1^{Cd*}}$  by  $\gamma^s$

and  $\frac{\sum_{a1}^{Cd} \bar{\phi}_1^{Cd} V_1^{Cd}}{\sum_{a1}^s \bar{\phi}_1^s V_1^s}$  by  $\frac{\gamma^s - 1}{\gamma^s}$ , the term may be approximated

as  $\frac{(\gamma^s - 1)^2}{\gamma^s}$ , which for gold is about 0.00022. Therefore, the third term of the denominator may be neglected in comparison with the others within the experimental precision expected.

Within these approximations  $Y$  may be expressed as:

$$Y = \left( \frac{\sum_{a2}^s \bar{\phi}_2^s}{\sum_{a1}^s \bar{\phi}_1^s} \right) \left\{ \frac{\gamma^s (p_s^{Cd} - p_o^{Cd})}{(p_s - p_o) - \gamma^s (p_s^{Cd} - p_o^{Cd})} \right\}$$



Substitution of these expressions for  $\left( \frac{\sum_{\alpha_1}^u \bar{\phi}_1^u V^u}{\sum_{\alpha_1}^s \bar{\phi}_1^s V^s} \right)$  and  $Y$  into

equation (A-1) gives:

$$\sum_{\alpha_2}^u = \sum_{\alpha_2}^s \left\{ \frac{\bar{\phi}_2^s V^s}{\bar{\phi}_2^u V^u} \right\} \left\{ \frac{(P_u - P_o) - Y^u (P_u^{cd} - P_o^{cd})}{(P_s - P_o) - Y^s (P_s^{cd} - P_o^{cd})} \right\} \quad (A-2)$$

It is to be noted that the ratio of the fast to slow neutron absorption rates does not appear in this equation.



## APPENDIX II

### COMPUTER PROGRAM FOR REDUCTION OF GOLD ACTIVATION DATA

The following Fortran 60 computer program, written by Associate Professor E. A. Milne, was utilized for computation of the gold foil specific activities.

```
DIMENSION D(100),C(100),R(100)
5 FORMAT (1H1,/21X,6HNUMBER,11X,7HWAITING,7X8HCOUNTING6X9HCORRECTED,
18X7HRATE AT/3X7HFOIL ID11X9HOF COUNTS8X4HTIME10X4HTIME10X4HRATE13X
26HTW = 0/)
10 FORMAT (3E10.5)
11 FORMAT (A8,A7,F10.0,3F10.5)
12 FORMAT (A8,A7,F15.0,4F15.5)
13 FORMAT (/20X16HTRAVERSE NUMBER I2/)
I = 1
J = 0
M = 1
WRITE OUTPUT TAPE 3 , 5
READ INPUT TAPE 2, 10, FLAM, TAU, BG
15 READ INPUT TAPE 2, 11, A,B,D(I),TC,TW,W
IF (D(I)) 99,99,16
16 C(I) = D(I)/TC
C(I) = C(I)/(1.0 - C(I)*TAU) - BG
R(I) = C(I)*EXP(F(FLAM*TW)/W
IF (I-M) 20,18,20
18 M = M 12
J = J 1
WRITE OUTPUT TAPE 3, 13, J
20 WRITE OUTPUT TAPE 3, 12, A,B,D(I),TW,TC,C(I),R(I)
I = I 1
GO TO 15
99 STOP
```













thesJ455  
An investigation of the feasibility of a



3 2768 002 10733 6  
DUDLEY KNOX LIBRARY